Journal of Materials Chemistry C

Accepted Manuscript

This article can be cited before page numbers have been issued, to do this please use: A. K. K. Srivastava, T. Vijayakanth, P. Divya, B. Praveenkumar, A. Steiner and B. Ramamoorthy, *J. Mater. Chem. C*, 2017, DOI: 10.1039/C7TC01758H.

ROYAL SOCIETY OF CHEMISTRY

rsc.li/materials-c

View Article Online
DOI: 10.1039/C7TC01758H

Journal Name

ARTICLE

Altering Polarization Attributes in Ferroelectric Metallo-Cavitands by Varying Hydrated Alkali-Metal Guest Cations†

Received 00th January 20xx,
Accepted 00th January 20xx

DOI: 10.1039/x0xx00000x

www.rsc.org/

Anant Kumar Srivastava,[a] Thangavel Vijayakanth,[a] Pillutla Divya,[c] B. Praveenkumar,*[,c] Alexander Steiner*[,d] and Ramamoorthy Boomishankar*[,a,b]

Supramolecular ferroelectrics have emerged as an exciting topic of research for both fundamental understanding and practical applications in the areas of energy and electronics. Here, we describe the synthesis of two metallo-cavitands $[\{M_4L_8(H_2O)_8\}\supset 9(H_2O)]\cdot 8(NO_3)\cdot x(H_2O)$ [M=Ni^{2+} (**1**) or Co^{2+} (**2**)] and demonstrate solid-state host-guest behavior and ferroelectricity in presence of various hydrated alkali metal cations (Hy-A) at their intrinsic voids. Due to the confinement effects of the cavitands, the degree of hydration observed for these alkali metal ions are on the upper side, especially the K^+, Rb^+ and Cs^+ ions show high hydration numbers of 8, 9 and 10, respectively. Ferroelectric studies on **1**, [Hy-A]⊂**1** and [Hy-A]⊂**2** assemblies show remnant polarization (P_r) values ranging from 27 to 30 μCcm^{-2} with concomitant variations in the coercive field (E_c) values at a lower frequency of 0.1 Hz. The observed features for the P-E loop characteristics of all the assemblies are reminiscent of triglycine sulphate (TGS) and certain other supramolecular ferroelectrics. Interestingly, ferroelectric fatigue measurements on all these systems show sizable variations as the cavitands with hard Li^+ ions exhibiting the maximum (fatigue) tolerance and the ones with higher polarizable Cs^+ ions show a reduction in P_r values up to 35%, after 10^5 switching cycles. The results signify the effect of encapsulated guest molecules in altering the polarization attributes (P_r, E_c and fatigue tolerance) via host-guest interactions.

Introduction

Ferroelectric substances are characterized by spontaneous electric polarization that can be reversed by the inversion of the applied electric field.[1] Ferroelectrics, owing to their electric switchable nature, are widely used as multifunctional electroactive polar materials for high-performance devices.[2-8] In addition to their great potential as memory elements, ferroelectric materials are actively been pursued for energy harvesting applications due to their piezoelectric and pyroelectric properties.[9-16] Ferroelectricity was first discovered in Rochelle salt,[17] but since then inorganic oxides (BTO and PZT, etc.) and polymers (PVDF and its copolymers) have been the desired choice of materials for ferroelectric applications.[18-21] Ferroelectricity has also been observed in certain supramolecular systems based on organic, liquid crystalline, charge-transfer and metal-organic scaffolds as they can possess specific advantages such as facile synthesis, low density, flexibility, and easy fabrication over the traditional ferroelectric inorganic oxides.[22-25] In most of these systems, supramolecular interactions that facilitate hydrogen displacement, coaxed charge-transfer complexation and dipole encapsulation etc. have contributed to their polar order. Nevertheless, inducing noncentrosymmetric polar packing arrangements in these systems is still challenging and serendipitous.

Recently, ferroelectric metal-organic and hybrid organic-inorganic materials have gained tremendous attention as the noncentrosymmetric arrangement of dipoles in these assemblies can be efficiently invoked by simple chemical modifications like nature of metal-ligand interactions, choice of cations and anions and the extra-framework molecules present in them.[26-34] In some instances, charge-balanced MOFs and molecular motion systems have been shown to exhibit ferroelectric ordering under the influence of an applied electric field.[35,36] In this effort, our group has synthesized a family of $\{Cu^{II}L_2\}_n$ based assemblies, derived from flexible dipodal ligands of the type $[PhPO(NHPy)_2]$, (Py = 2-pyridyl (^{2}Py) or 3-pyridyl (^{3}Py) or 4-pyridyl(^{4}Py)), which showed noncentrosymmetric structure and subsequent ferroelectric responses depending on the counter anions, dimensionality of the framework and solvate molecules present in them.[37,39] These findings prompted us to look for a robust $\{M^{II}L_2\}_n$ system based on these ligands in which the ferroelectric polarization attributes can be systematically altered by using certain

[a] Department of Chemistry, Indian Institute of Science Education and Research (IISER), Pune, Dr. Homi Bhabha Road, Pune – 411008, India. *Email: boomi@iiserpune.ac.in
[b] Centre for Energy Science, Indian Institute of Science Education and Research (IISER), Pune, Dr. Homi Bhabha Road, Pune – 411008, India.
[c] Armament Research and Development Establishment, Dr. Homi Bhabha Road, Pune – 411021, India. *Email: praveenkumar@arde.drdo.in
[d] Department of Chemistry, University of Liverpool, Crown Street, Liverpool – L69 7ZD, United Kingdom. *Email: A.Steiner@liverpool.ac.uk

†Electronic Supplementary Information (ESI) available: [CCDC 1543622-1543633 contains the supplementary crystallographic data. Experimental details, additional figures and tables pertaining to crystal structures, PXRD, dielectric and ferroelectric measurements]. See DOI: 10.1039/x0xx00000x

chemically tunable functions. Specifically, we paid attention to obtain discrete ferroelectric metal-ligand cages and cavitands and to get insights on certain supramolecular interactions or host-guest behaviour that influences the overall polarization in them.

Herein, we report the synthesis of two noncentrosymmetric cavitands of formula $[\{Ni_4L_8(H_2O)_8\}\supset 9(H_2O)]\cdot 8(NO_3)\cdot 25(H_2O)$ (**1**) and $[\{Co_4L_8(H_2O)_8\}\supset 9(H_2O)]\cdot 8(NO_3)\cdot 27(H_2O)$ (**2**), built on the phosphoramide ligand L, $PhPO(NH^3Py)_2$. Owing to the presence of large intrinsic cavities, host-guest systems based on hydrated alkali metal cations (Hy-A), ranging from Li^+ to Cs^+ ions has been synthesized for both **1** and **2**. Structural analyses revealed that the hydration spheres around the alkali metal ions were found to be on the higher side, especially the K^+, Rb^+ and Cs^+ ions were exclusively coordinated with 8, 9 and 10 molecules of water, respectively. Ferroelectric hysteresis measurements on **1** gave a well-saturated loop with high remnant polarization (P_r) value of 29.50 μCcm^{-2} (at 0.1 Hz). The P-E loop measurements on all the (Hy-A)⊂**1** and (Hy-A)⊂**2** systems show excellent ferroelectric responses with notable variations in their polarization attributes, which are consistent with the polarizability of the alkali metal cations. Interestingly, the ferroelectric fatigue measurements on (Hy-A)⊂**1** and (Hy-A)⊂**2** systems show exceptional fatigue resistant behaviour albeit with a prominent reduction in P_r for the Cs-encapsulated systems at higher switching cycles. These observations suggest the effect of intrinsic-guest molecules in the overall polarization of the $\{M_4L_8\}^{8+}$ cavitand systems. To the best of our knowledge, the present study is unique of its kind for the systematic investigation on a family of supramolecular host-guest systems.

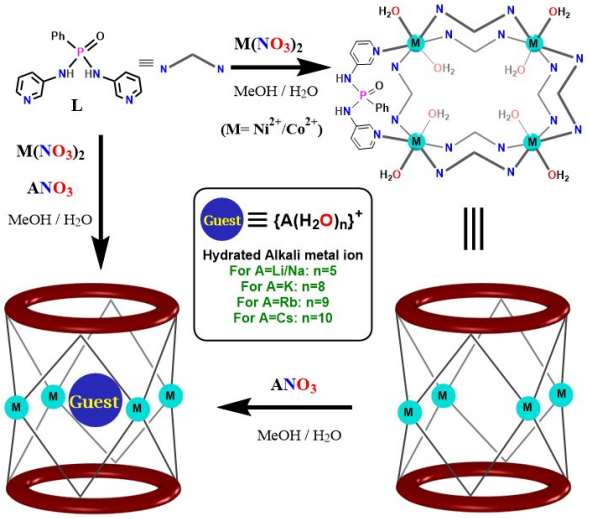

Scheme 1. Schematic diagram for obtaining the tetrameric Ni/Co-cavitands and their hydrated alkali metal ion encapsulated systems.

Results and discussion

Synthesis

The Ni_4-cavitand **1** was isolated as blue coloured crystals in a 2:1 reaction mixture involving L (prepared by our reported procedure)[38] and $Ni(NO_3)_2\cdot 6H_2O$ in $MeOH/H_2O$ medium at room temperature (Scheme 1). Performing the reaction in the presence of alkali metal cations (A^+), employed as their corresponding nitrate salts, results in the formation of the host-guest systems [Hy-A]⊂**1** and [Hy-A]⊂**2** (where [Hy-A]= $[A(H_2O)_n]^+$; for A = Li/Na n = 5; for A = K/Rb/Cs: n = 8/9/10). A similar reaction of L with $Co(NO_3)_2\cdot 6H_2O$ in $MeOH/H_2O$ results in the corresponding the Co_4-cavitand **2**, in low yields. However, the yields of the {[Hy-A]⊂**2**} systems drastically increase when the reaction was performed in the presence of alkali metal nitrate salts (Scheme 1).

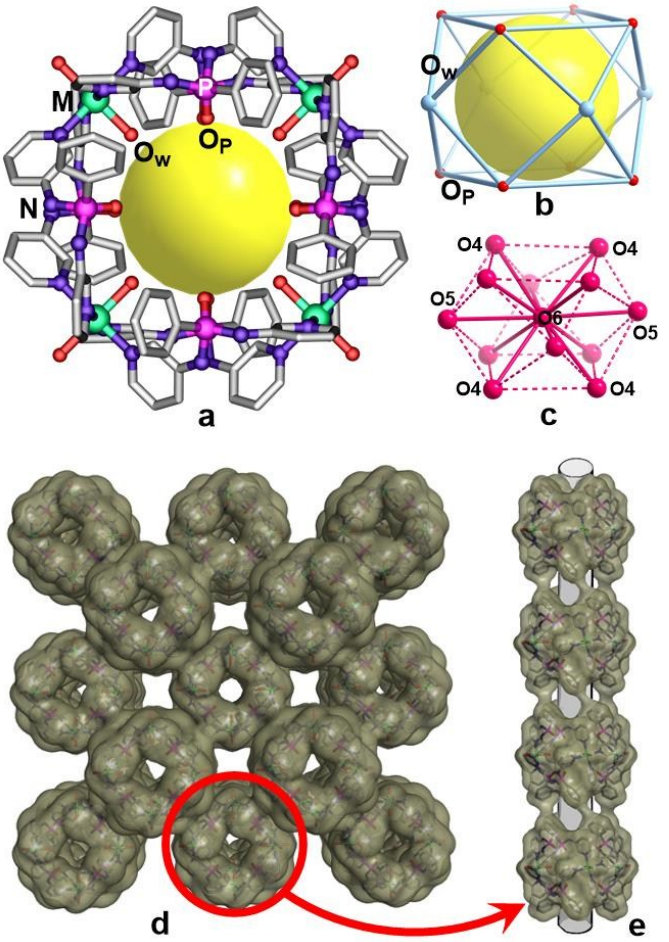

Fig. 1. (a) View of the tetrameric core in **1** and **2**. (b) The cuboctahedral cavity and (c) the cuboctahedral arrangement of the solvate molecule in them. (d) The bcc packing along the c-axis. (e) View of a 1D-channel like structure that connects the intrinsic cavities.

Crystal Structures of 1 and 2

The crystal structures of **1** and **2** were solved in the tetragonal space group *I422* (symmetry *D4*). The molecular structures of both **1** and **2** consist of a cationic metal-ligand core, disordered nitrate ions and encapsulated solvate molecules. The metal ions in them were located in a distorted octahedral geometry, consisting of four $N_{pyridyl}$ planar contacts and two axially coordinated water molecules. The structures can be described as tetranuclear M_4L_8 cavitands built from four edge-shared 20-membered macrocyclic M_2L_2 segments (Fig. 1a). The metal ions

View Article Online
DOI: 10.1039/C7TC01758H

were found to be located at the corners of a square plane and each of the four bidentate ligand pairs sit above and below the M_4-plane. The two $N_{pyridyl}$ functionalities in each of the ligand motifs were aligned in *syn*-conformation with respect to the endo oriented P=O groups. The inner surfaces of the cavitands were lined with O-atoms from eight phosphoramide ligands (O_P) and four Ni-bound water molecules (O_W) that are arranged at the corners of a putative distorted cuboctahedron (Fig. 1b, Fig. S3, ESI). These intrinsic voids were filled with nine disordered water molecules. One of them (O6) is unique and is located at the centre of the cage. The remaining ones, O4 and O5 (disordered) occupy the peripheral positions giving rise to another H-bonded cuboctahedron (Fig. 1c).

The unit-cell diagrams of both **1** and **2** show the presence of solvent accessible extrinsic voids (in addition to the intrinsic voids) that are lined up with nitrate anions and bulk of solvate molecules (Fig. 1d, Fig. S4, ESI). In both **1** and **2**, the tetragonal body-centered packing facilitates the stacking of the cavitands one below the other in an eclipsed manner. This arrangement leads to the formation of a contiguous one-dimensional pore resembling a nano-channel like structure that runs parallel to the long c-axis (Fig. 1e, Fig. S5, ESI). In case of the previously reported Cu_4L_8 cavitand, the adjacent layers, as well as the one below other, are orthogonally arranged with respect to each other (Fig. S6, ESI).[38] Such an arrangement precludes the extension of their voids as 1D-channels in the Cu_4L_8 cavitand.

Crystal Structures of the Host-Guest Assemblies

The single crystal X-ray diffraction (SCXRD) analysis on the {[Hy-A]⊂**1**} and {[Hy-A]⊂**2**} assemblies confirmed the encapsulation of corresponding $[A(H_2O)_n]^+$ motifs in all of them while retaining the parent tetrameric structures (Fig. 2a). Since both the {[Hy-A]⊂**1**} and {[Hy-A]⊂**2**} assemblies are iso-structural in most instances, henceforth all the molecular structure descriptions are presented only with respect to the {[Hy-A]⊂**1**} systems for the sake of simplicity. All the [Hy-A] encapsulated structures contain a large electron density peak at the central position of the cage (Wyckoff site 2a) except that of {[Hy-Na]⊂**2**}. In cases of {[Hy-Li]⊂**1**}, and {[Hy-Na]⊂**1**, this peak can be attributed to a water molecule as found in **1** (O6). In these assemblies, the Li^+ and Na^+ ions are located along the four-fold axes away from the central position of O6 and generate meaningful distances to O4 (aqua ligands). As a result, Li and Na atoms would have to be disordered over the two equivalent positions along the 4-fold axis. The metal ions have square-pyramidal environments (Fig. 2b and 2c); the water molecule at their apex may be the one that occupies the equivalent site (O7 in case of Na) or the one at the central position (O6 in case of Li) (Fig. S7 and S8, ESI). Considering the low occupancy factors of Na (1/4) in {[Hy-Na]⊂**1**}, the scenario of the hosted metal ion (Fig. S8a, ESI) may co-exist with the one that features no metal ion but only a water molecule at the center of the cage (Fig. S8b, ESI). Observation of such $A(H_2O)_5$ motifs are unprecedented in the family of hydrated Li^+ and Na^+ ions. In fact for the Li^+ ions, the tetrahedral $[Li(H_2O)_4]$ coordination has been shown to be energetically favoured over the $[Li(H_2O)_5]$ geometry.[40] In this regard, the present findings indicate that the M_4-cavitands not only efficiently encapsulate Li^+ ion but also stabilizes the energetically less favoured $[Li(H_2O)_5]^+$ system.

The heavier alkali metal ions K^+, Rb^+ and Cs^+ occupy the center of the cage (in place of O6 at the Wyckoff site 2a); their coordination environment is determined by the relative occupancy of positions of the water shell. Altogether there are twelve positions for O4 and O5 in a cuboctahedral arrangement around the center of the cage (Fig. 2g). The disordered state produces a 24 vertex truncated cube as the positions of O4 are also disordered in these structures in addition to the disorder of the O5 positions as observed before (Fig. S9, ESI). Since O_P atoms are exclusively H-acceptors and O_M sites are H-donors, there are only a few arrangements possible which would generate an appropriate H-bonded network such as the cuboctahedral one observed for **1**.

In order to extract the exact hydration number for these $K^+/Rb^+/Cs^+$ ions, refinements for their corresponding structures were performed with varying hydration numbers ranging from 6 to 12. From these refinement data, coordination numbers of 8, 9 and 10 for K^+, Rb^+ and Cs^+ ions, respectively (Fig. 2d-f), appear to be in good agreement with the listed values (Table S2 and S3, rows highlighted in yellow, ESI). While the most favoured coordination for these heavier cations is only seven (for K) or eight (for Rb and Cs) in bulk aqueous systems,[41] the higher hydration spheres observed for the $K^+/Rb^+/Cs^+$ assemblies is a consequence of the confinement effects. Moreover, there is a very little information available on the hydration spheres of Rb^+ and Cs^+ ions because of their low charge densities.[42,43] Furthermore, the A-O distance between $O_{hydrated}$ (O4 and O5) and the alkali metal ions show a slight increase from K to Cs. However, the O-O distances pertaining to $O_{hydrated}$ and O_P or O_w are fairly similar for all of them, and are in the appropriate range for hydrogen bonding (Table S4, ESI). The packing diagrams of all the {[Hy-A]⊂**1**} and assemblies closely resemble to that of **1** and the guest encapsulated tetrameric cores in them were again stacked in an eclipsed manner along the 4-fold axis (Fig. 2h). This arrangement results in a one-dimensional array of H-bonded alkali metal framework inside the non-covalent channels of **1**.

Ferroelectric and Dielectric Studies on 1

The ferroelectric hysteresis measurements on **1** gave a well saturated polarization vs. electric field (P-E) loop at low frequencies (Fig. 3a, Fig. S10, ESI). A remnant polarization (P_r) value of 29.50 μCcm^{-2} has been observed at a lower frequency of 0.1 Hz (29.06 μCcm^{-2} at 1 Hz). Also, the coercive fields (E_c) were obtained at 8.60 (0.1 Hz) and 12.35 $kVcm^{-1}$ (1 Hz) which are much smaller than many commercial ferroelectric materials such as PVDF. This is attributed to the facile switching of the polarizable domains in **1**, a desired property for many practical applications. Further, from the obtained leakage current densities (ranges between 10^{-4} and 10^{-9} Acm^{-2}) and the frequency dependent conductivity plots (ranges between 10^{-4} and 10^{-12} Scm^{-1}), the ferroelectric origin of the hysteresis loops in **1** can be confirmed (Fig. S11 and S12, ESI). Also, the ferroelectric fatigue studies were performed on **1** to

View Article Online
DOI: 10.1039/C7TC01758H

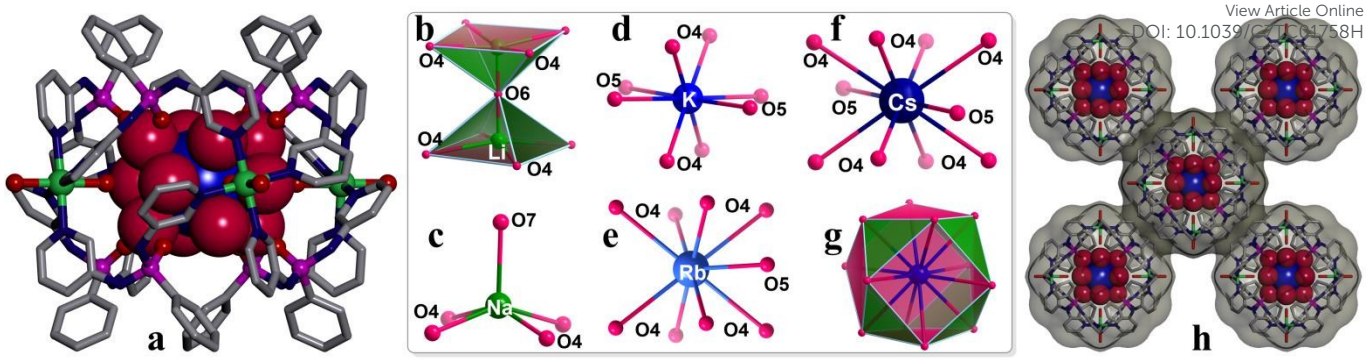

Fig. 2. (a) Molecular structure of [Hy-K]⊂**1**. (b) The disordered $[Li(H_2O)_5]^+$ fragments in the square pyramidal geometry. (c)-(f) View of the respective idealized core geometries of $[Na(H_2O)_5]^+$, $[K(H_2O)_8]^+$, $[Rb(H_2O)_9]^+$ and $[Cs(H_2O)_{10}]^+$ ions. (g) The cuboctahedral arrangement of the O4 and O5 atoms around $K^+/Rb^+/Cs^+$ ions. (h) The packing view of [Hy-K]⊂**1** along the c-axis.

verify the retention of polarization after several bipolar switching cycles. These studies show a remarkable fatigue resistant behaviour as its P_r values (at 1 Hz) remained almost same even after 10^5 cycles (Fig. 3b). This suggests the absence of space charge accumulation (or movement) and reduction in the pinning of domain walls, which ultimately aids in the facile switching of its polarizable domains and confirms the ferroelectric origin of the obtained loop.[44] Furthermore, the stability of the compound **1** during P-E loop measurements was confirmed by the PXRD analysis which gave similar peak profiles for the sample before and after ferroelectric measurements (Fig. S13, ESI).

Since the tetrameric cavitands in **1** and **2** exhibit a crystallographic '422' nonpolar point group, the observed P-E loop hysteresis for **1** is thus believed to originate from the array of the encapsulated solvates at the intrinsic nano-channels (Fig. 3e).[45] This observation can be supported by earlier studies on the ordered arrangement of polar solvents within the nanosized ensembles such as carbon nanotube, nanopore membranes and porous framework solids which have shown to induce ferroelectric polarization in presence of an external field.[46-49] This was verified by subjecting the sample of **1** to a forward electric field from 0.1 to 15 $kVcm^{-1}$ which gave the P-E loops with a progressively improved shape and saturation polarization. A closer look at the P-E loops in the forward sweep between 9.32 and 10.68 $kVcm^{-1}$ indicates that the threshold field with which the dipoles in **1** can be completely aligned is attained at 10.68 $kVcm^{-1}$ (Fig. 3c). However, the shape and the polarization values of the P-E loops were retained in the backward sweep of the field until 9.32 $kVcm^{-1}$ (Fig. 3d). This implies that once the dipoles are fully aligned (at the threshold field), the maximum P_r and P_s values along with the shapes of the loops can be retained even at certain lower electric fields. Thus **1** exhibits electric field induced realignment of the dipoles that originates from the ordering of the polar guest-molecules. Such a behaviour has been observed in certain ceramic and supramolecular ferroelectric materials as well.[35,50,51] Dipole moment (ONIOM) calculations performed on the assembly of **1** show that almost 60% of the polarizable dipoles in **1** originates from the intrinsic guest solvates (Table S5, ESI). These observations consistent with the P-E loop obtained on the desolvated samples of 1 and which gave negligible polarization (Fig. S14, ESI). Similar P-E loop measurements could not be performed on **2** owing to the poor yields of its crystals in the absence of template guest molecules (vide infra). The reported P_r and E_c values of **1** are the best among the class of supramolecular compounds (Table S6, ESI).[23,52-58] The observed trend in the P_r and P_s values and the shape of the loops in **1** are reminiscent to that of TGS (though these values are much higher for **1**). This can be attributed to higher relaxation time necessary for the alignment of dipoles that are held together by weak interactions such as H-bonding. Such behaviour is found to be common among several supramolecular ferroelectrics.[59]

The temperature dependent dielectric measurement on **1** at various frequencies gave an anomalous peak at 40 °C with a maximum ε' (real part of permittivity) value of 73.9 at 100 Hz (Fig. 3f). The broad feature of the anomaly peaks, at a relatively low-temperature, indicates the presence of desolvation-assisted phase transition in **1**. At higher frequencies, the broad anomalous peak was found to be slightly shifted to higher temperatures along with a decrease in the maxima of its ε' values. Such shift in peak intensities were observed for both ε'' (imaginary part of permittivity) and tan-δ (dielectric loss) parts as well with an opposite shift in its intensity maxima (Fig. 3g, Fig. S15, ESI). These observations

View Article Online DOI: 10.1039/C7TC01758H

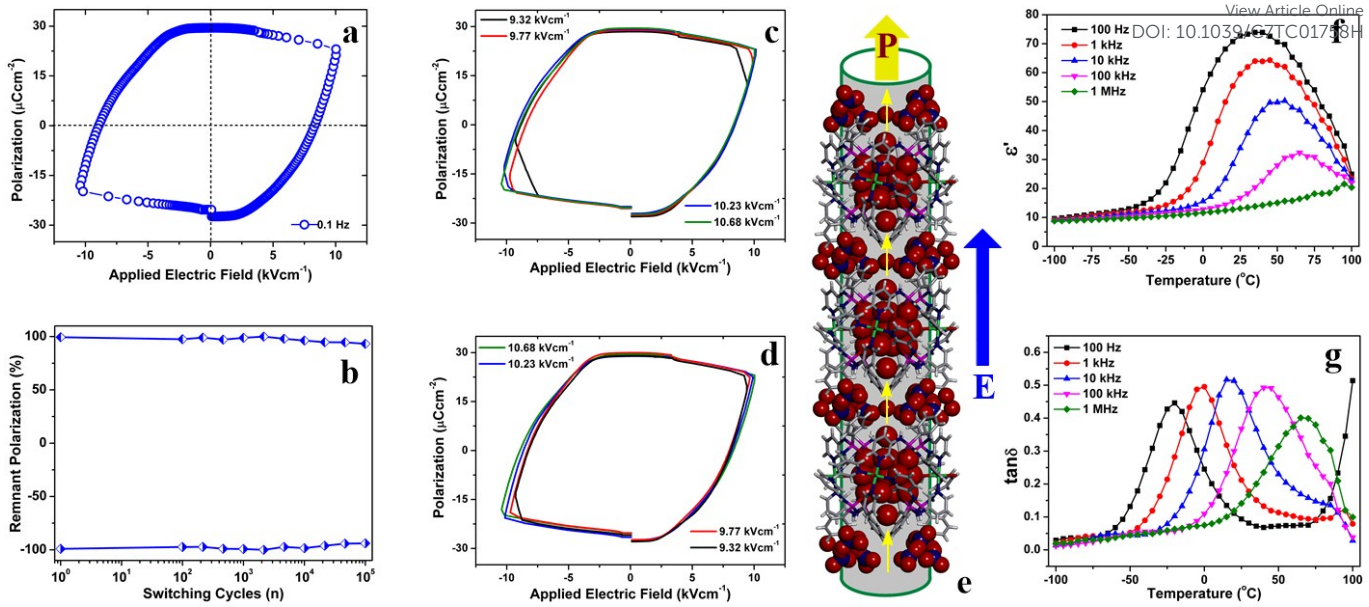

Fig. 3. (a) Ferroelectric hysteresis loop of **1** and (b) its fatigue data up to 10^5 cycles at 1 Hz. (c) and (d) Evolution of the P-E loops of **1** at the various fields in the forward and backward sweeps, respectively. (e) Schematic depicting the ordering of the confined guest molecules under the external field. Temperature dependence of (f) the real part of dielectric constant and (g) dielectric loss of **1** at various frequencies showing the dielectric relaxation phenomenon.

can be compared to the trend observed for typical relaxor materials[60,61] and in the present instance it can be attributed to the desolvation assisted dielectric relaxation phenomenon. The differential scanning calorimetry (DSC) measurements on **1** gave no peaks in the temperature range of -50 to 100 ˚C which suggests that the observed broad dielectric anomaly peak does not corresponds to any phase (structural) transition, rather is associated with the release of solvates from **1**.

Ferroelectric and Dielectric Studies of {[Hy-A]⊂M_4} systems

Subsequent ferroelectric measurements on both {[Hy-A]⊂**1**} and {[Hy-A]⊂**2**} systems resulted in a well saturated rectangular P-E loops for almost all the host-guest assemblies (except for [[Hy-Na]⊂**1**])[62] with slight variation in their P_r and E_c values at 1 Hz (Fig. 4a-b). From Fig. 4a, it can be observed that there is a marginal decrease and increase in the P_r values for {[Hy-Li]⊂**1**]} and {[Hy-Cs]⊂**1**]}, respectively, whereas the E_c values were found to be showing values in an opposite trend for these two systems. The {[Hy-K]⊂**1**]} and {[Hy-Rb] ⊂**1**]} systems show a nearly similar P_r and E_c values and lies in-between those of {[Hy-Li]⊂**1**]} and {[Hy-Cs]⊂**1**]} (Fig. 4c). This signifies that the hardness and softness of the alkali-metal ions, which is related to the size and strength of their polarizability, plays a vital role in the alignment of their dipoles. Thus, the comparably higher E_c value for {[Hy-Li]⊂**1**]} over **1** and other {[Hy-A]⊂**1**]} systems can be attributed to the hardness of the Li^+ ion, which requires relatively higher fields to achieve the maximum polarization. However, the presence of softer K, Rb and Cs cations in **1** facilitates a swift polarization switching at relatively lower electric fields compared to [Hy-Li]⊂**1**. A similar trend can be observed for the {[Hy-A]⊂**2**]} assemblies as well, albeit with a slightly less prominent shifts in their P_r and E_c values (Fig. 4b-c). All these observations corroborate the role of alkali-metal guest cations on the overall polarization of these systems.

To further check the effect of guest encapsulation on the polarization properties of the host-guest systems, the temperature dependent dielectric permittivity measurements were performed on all the {[Hy-A]⊂**1**} and {[Hy-A]⊂**2**} systems (Fig. S16 and S17, ESI). Thus, all the guest-encapsulated systems of the Ni_4- and Co_4-series show nearly similar ε' values (within their series) at all the measured frequencies and the obtained values are comparable with that of **1**. The dielectric anomaly peaks for the Ni_4- and Co_4-series were comparable to each other and ranges from 35 to 40 °C and their ε' values were ranging between 60 and 75 at 1 kHz. Again the P-E loop measured on the desolvated samples of {[Hy-Li]⊂**1**]} and {[Hy-Cs]⊂**1**]} show negligible polarization. This emphasises the effect of hydrated solvates in governing the polarizable dipoles in the host-guest systems (Fig. S18, ESI).

View Article Online
DOI: 10.1039/C7TC01758H

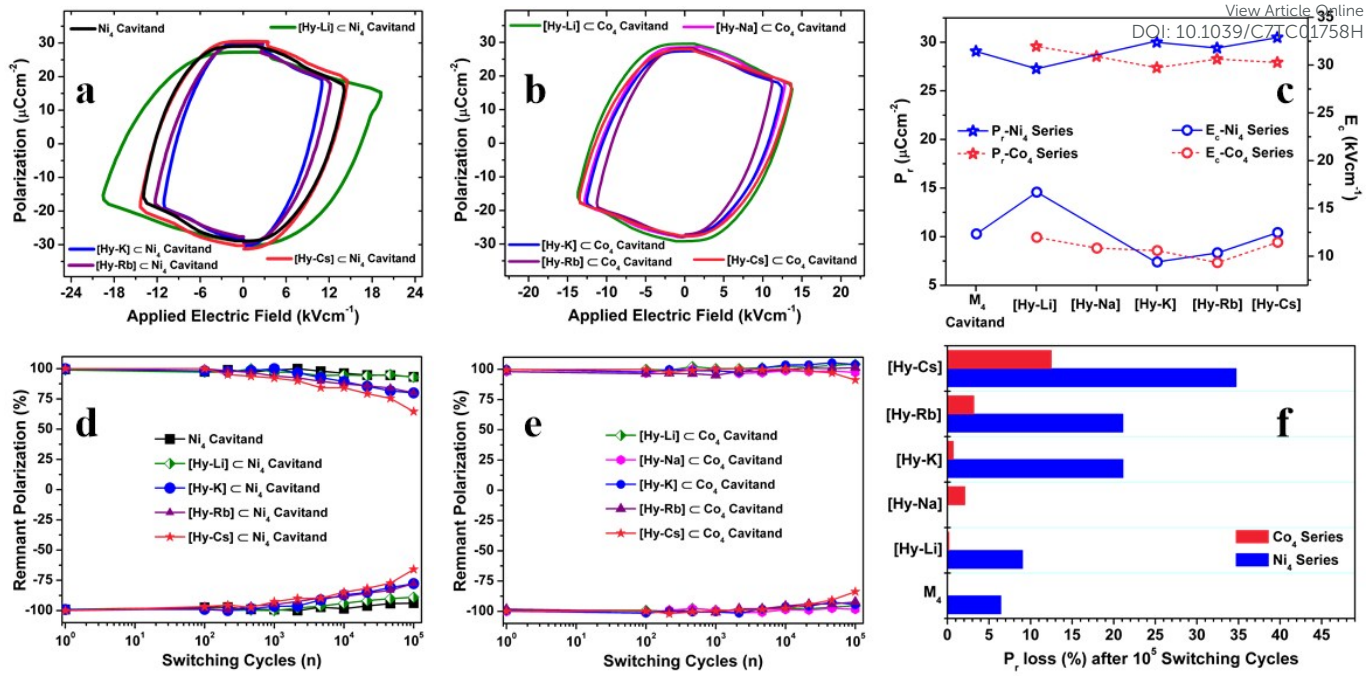

Fig. 4. Ferroelectric P-E loops of (a) {[Hy-A]⊂**1**} and (b) {[Hy-A]⊂**2**} systems at 1 Hz and (c) the comparison of their P_r and E_c values. Ferroelectric fatigue data for all the (d) {[Hy-A]⊂**1**} and (e) {[Hy-A]⊂**2**} systems at 1 Hz and (f) the averaged P_r reduction values (%) after 10^5 switching cycles.

The fatigue measurements showed an interesting trend, yet with a high P_r after 10^5 cycles, for all these host-guest assemblies. Notably, for the Ni_4-series, the fatigue tolerance of the guest-encapsulated systems (except that of Li^+), was found to decrease beyond 10^4 cycles as the size of the alkali metal cation increases. The fatigue studies of the Co_4-series also show a very similar trend but with a less pronounced reduction in P_r at higher switching cycles. Interestingly from the Fig. 4d and 4e, it can be observed that the Li^+ encapsulated systems, {[Hy-Li]⊂**1**]} and {[Hy-Li]⊂**2**]}, exhibited the best fatigue resistant behaviour among all of them. This shows that these assemblies can exhibit a longer polarization memory, once the smaller and hard Li^+ ions are polarized under an external electric field. The guest assemblies with the bigger (and soft) Cs^+ ions, {[Hy-Cs]⊂**1**]} and {[Hy-Cs]⊂**2**]}, were the most fatigue prone systems as their respective P_r at 1 Hz have been pruned to 65% and 87% of the original values, after 10^5 cycles (Figure 4f). The reduction of polarization for the [Hy-Cs] systems at higher cycles, despite the presence of polarizable Cs^+ ions, can be attributed to its size and compact fitting within the cavitand structure.

Thus the [Hy-Cs] moieties, owing to their efficient host-guest complexation, may exhibit a restricted orientation for the switchable domains during the bipolar cycles. The other K^+ and Rb^+ encapsulated systems showed an intermediate fatigue tolerance among their series and again the Co_4-derived systems showing a better retention of P_r in comparison with the Ni_4-based systems (Fig. 4f, Table S7, ESI). All these results suggest that the encapsulation of hydrated alkali metal ions at the intrinsic cavities exhibits a clear influence on the polarization attributes of the M_4-cavitands. Also, from the shapes of the P-E loops and from the fatigue studies it can be gleaned that the Co_4-cavitand of **2** provides a better and efficient platform over the Ni_4-cavitand of **1** for an overall and robust polarization. In this context, it can be noted that change of metal ions have shown to alter the ferroelectric polarization in metal-formate based 3D-frameworks.[63] Thus, it is reasonable to visualize that the change of metal ions (both host and guest) has a clear influence on the overall polarization attributes of the {[Hy-A]⊂**M_4**]}systems.

Conclusions

This work presents a comprehensive study on the ferroelectric behaviour of a family of Ni_4L_8 and Co_4L_8 cavitands that are crystallized in the tetragonal symmetry. These cavitands are packed in a body-centered crystal lattice and show a non-covalently stacked 1D-columnar like structure for their intrinsic cavities. The inner space of these cavitands provides cuboctahedral pockets that host a series of hydrated alkali metal cations. The lighter Li^+ and Na^+ ions were disordered and exist as penta-hydrates in distorted square pyramidal geometry. Also, this is the first instance for the observation of thermodynamically less favourable $[Li(H_2O)_5]^+$ motifs. The heavier K^+, Rb^+ and Cs^+ ions take up the general position and have highest hydration spheres of 8, 9 and 10 molecules of water, respectively. The observed highest coordination for these heavier cations can be attributed to the hydrophilic as well as the confinement effects of the voids. Ferroelectric measurement on **1** shows an excellent ferroelectric P-E hysteresis loop with a remnant polarization of 29.50 μCcm^{-2}. Remarkably, all the {[Hy-A]⊂**M_4**]} systems were shown to retain the high polarization due to **1** with some variations in the P_r and E_c values. However, ferroelectric fatigue data

obtained on all the {[Hy-A]⊂**M₄**]} show sizable variations among these assemblies for the P_r values, after 10^5 switching cycles, that can be related to the differences in polarizability and size of the encapsulated cations. Thus, the {[Hy-Li]⊂**2**]} assembly containing the least polarizable Li^+ ion exhibits the highest fatigue resistance while the {[Hy-Cs]⊂**1**]} showing a drop of about 35% in the P_r value. These observations highlight the prominence of host-guest systems in the domain of ferroelectric materials and signify the effect of supramolecular interactions on the polarization attributes such as spontaneous polarization, coercive fields and fatigue tolerance. Ferroelectric supramolecules, owing to their facile synthesis, solution viability and low temperature processability, has an excellent prospect as a new class of materials for high-tech applications in the years to come. Such supramolecular ferroelectrics are envisioned to be worthwhile materials for fabricating flexible nanogenerators[64] and other energy harvesting systems.

Acknowledgements

This work was supported by SERB, India via Grant No. EMR/2016/000614 (R.B.) and Nanomission Project, DST, India via Grant No. SR/NM/TP-13/2016. A.K.S. thanks the CSIR, India and T. V. thank the UGC, India for the fellowship.

References

1 M. E. Lines and A. M. Glass, *Principles and Applications of Ferroelectrics and Related Materials*, Oxford University Press, New York, 1977.
2 J. F. Scott, *Ferroelectric memories*, Vol. 3, Springer Science & Business Media, Heidelberg, Germany, 2000.
3 K. Uchino, *Ferroelectric Devices*, 2nd ed., CRC Press, Boca Raton, FL, USA, 2009.
4 Y. Xu, *Ferroelectric materials and their applications*, Elsevier, Amsterdam, 2013.
5 S. Das and J. Appenzeller, *Nano Lett.*, 2011, **11**, 4003-4007.
6 R. Whatmore, *Ferroelectric Materials*, In *Springer Handbook of Electronic and Photonic Materials*, Springer, 2007, 597-623.
7 J. F. Scott, *Science*, 2007, **315**, 954-959.
8 G. A. Smolenskii, V. A. Bokov, V. A. Isupov, N. N. Krainik, R. E. Pasinkov and I. A. Sokolov, *Ferroelectrics and Related Materials*, Gordon and Breach Science Publishers, New York, 1984.
9 K. M. Ok, E. O. Chi and P. S. Halasyamani, *Chem. Soc. Rev.*, 2006, **35**, 710-717.
10 Y. Zhang, M. Xie, J. Roscow, Y. Bao, K. Zhou, D. Zhang and C. R. Bowen, *J. Mater. Chem. A*, 2017, **5**, 6569-6580.
11 C. Wan and C. R. Bowen, *J. Mater. Chem. A*, 2017, **5**, 3091-3128.
12 M. Xiea, S. Dunnb, E. L. Boulbarc and C. R. Bowen, *Int. J. Hydrogen Energy*, 2017. (In Press; DOI: 10.1016/j.ijhydene.2017.02.086)
13 J. Roscow, Y. Zhang, J. Taylor and C.R. Bowen, *Eur. Phys. J. Special Topics*, 2015, **224**, 2949–2966.
14 C. R. Bowen, J. Taylor, E. LeBoulbar, D. Zabek, A. Chauhan and R. Vaish, *Energy Environ. Sci.*, 2014, **7**, 3836–3856.
15 B. Chen, J. Shi, X. Zheng, Y. Zhou, K. Zhuc and S. Priya, *J. Mater. Chem. A*, 2015, **3**, 7699-7705.
16 Z. Fan, K. Sun and J. Wang, *J. Mater. Chem. A*, 2015, **3**, 18809–18828.
17 J. Valasek, *Phys. Rev.*, 1921, **17**, 475-481.
18 G. H. Haertling, *J. Am. Ceram. Soc.*, 1999, **82**, 797-818.
19 T. A. Vanderah, *Science*, 2002, **298**, 1182-1184.
20 T. Furukawa, M. Date and E. Fukada, *J. Appl. Phys.*, 1980, **51**, 1135–1141.
21 T. Furukawa, *Phase Trans.*, 1989, **18**, 143–211.
22 A. S. Tayi, A. Kaeser, M. Matsumoto, T. Aida and S. I. Stupp, *Nat. Chem.*, 2015, **7**, 281-294.
23 S. Horiuchi and Y. Tokura, *Nat. Mater.*, 2008, **7**, 357-366.
24 S. Ghosh, D. D. Sante and A. Stroppa, *J. Phys. Chem. Lett.*, 2015, **6**, 4553-4559.
25 P. Jain, V. Ramachandran, R. J. Clark, H. D. Zhou, B. H. Toby, N. S. Dalal, H. W. Kroto and A. K. Cheetham, *J. Am. Chem. Soc.*, 2009, **131**, 13625-13627.
26 W. Zhang and R.-G. Xiong, *Chem. Rev.*, 2012, **112**, 1163-1195.
27 T. Hang, W. Zhang, H.-Y. Ye and R.-G. Xiong, *Chem. Soc. Rev.*, 2011, **40**, 3577-3598.
28 W. Zhang, H.-Y. Ye and R.-G. Xiong, *Coord. Chem. Rev.*, 2009, **253**, 2980-2997.
29 P.-F. Li, Y.-Y. Tang, Z.-X. Wang, H.-Y. Ye, Y.-M. You and R.-G. Xiong, *Nat. Commun.*, 2016, **7**, 13635-366.
30 P.-P. Shi, Y.-Y. Tang, P.-F. Li, H.-Y. Ye and R.-G. Xiong, *J. Am. Chem. Soc.*, 2017, **139**, 1319–1324.
31 Y.-Y. Tang, W.-Y. Zhang, P.-F. Li, H.-Y. Ye, Y.-M. You and R.-G. Xiong, *J. Am. Chem. Soc.*, 2016, **138**, 15784–15789.
32 H.-Y. Ye, J.-Z. Ge, Y.-Y. Tang, P.-F. Li, Y. Zhang, Y.-M. You and R.-G. Xiong, *J. Am. Chem. Soc.*, 2016, **138**, 13175–13178.
33 D. D. Sante, A. Stroppa, P. Jain and S. Picozzi, *J. Am. Chem. Soc.*, 2013, **135**, 18126-18130.
34 A. Stroppa, D. D. Sante, P. Barone, M. Bokdam, G. Kresse, C. Franchini, M.-H. Whangbo and S. Picozzi, *Nat. Commun.*, 2014, **5**, 5900.
35 T. Akutagawa, H. Koshinaka, D. Sato, S. Takeda, S.-I. Noro, H. Takahashi, R. Kumai, Y. Tokura and T. Nakamura, *Nat. Mater.*, 2009, **8**, 342-347.
36 D.-W. Fu, W. Zhang, H.-L. Cai, Y. Zhang, J.-Z. Ge, R.-G. Xiong and S. D. Huang, *J. Am. Chem. Soc.*, 2011, **133**, 12780-12786.
37 A. K. Srivastava, P. Divya, B. Praveenkumar and R. Boomishankar, *Chem. Mater.*, 2015, **27**, 5222-5229.
38 A. K. Srivastava, B. Praveenkumar, I. K. Mahawar, P. Divya, S. Shalini and R. Boomishankar, *Chem. Mater.*, 2014, **26**, 3811-3817.
39 R. Boomishankar and A. K. Srivastava, *Phosphorus, Sulfur, and Silicon and the Related Elements*, 2016, **191**, 618-623.
40 C. C. Pye, *Int. J. Quantum Chem.*, 2000, **76**, 62-76.
41 J. Mähler and I. Persson, *Inorg. Chem.*, 2012, **51**, 425-438.
42 T. Ikeda and M. Boero, *J. Chem. Phys.*, 2012, **137**, 041101.
43 F. Pichierri, *Dalton. Trans.*, 2013, **42**, 6083-6091.
44 C. W. Law, K. Y. Tong, J. H. Li and K. Li, *Solid-State Electron.*, 2000, **44**, 1569-1571.
45 L. Pan, G. Liu, H. Li, S. Meng, L. Han, J. Shang, B. Chen, A. E. Platero-Prats, W. Lu, X. Zou and R.-W. Li, *J. Am. Chem. Soc.*, 2014, **136**, 17477-17483.
46 H.-X. Zhao, X.-J. Kong, H. Li, Y.-C. Jin, L.-S. Long, X. C. Zeng, R.-B. Huang and L.-S. Zheng, *Proc. Natl. Acad. Sci. U.S.A.*, 2011, **108**, 3481–3486.
47 G. Menzl, J. Köfinger and C. Dellago, *Phys. Rev. Lett.*, 2012, **109**, 020602.
48 C.-F. Luo, W. Fa, J. Zhou, J.-M. Dong and X.-C. Zeng, *Nano Lett.*, 2008, **8**, 2607-2612.
49 X.-Y. Dong, B. Li, B.-B. Ma, S.-J. Li, M.-M. Dong, Y.-Y. Zhu, S.-Q. Zang, Y. Song, H.-W. Hou and T. C. W. Mak, *J. Am. Chem. Soc.,* 2013, **135**, 10214-10217.
50 J. Harada, T. Shimojo, H. Oyamaguchi, H. Hasegawa, Y. Takahashi, K. Satomi, Y. Suzuki, J. Kawamata and T. Inabe, *Nat. Chem.*, 2016, **8**, 946-952.
51 Q. Ke, W. Lu, X. Huang and J. Wang, *J. Electrochem. Soc.*, 2012, **159**, G11-G14.

View Article Online
DOI: 10.1039/C7TC01758H

52 S. Horiuchi, Y. Tokunaga, G. Giovannetti, S. Picozzi, H. Itoh, R. Shimano, R. Kumai and Y. Tokura, *Nature*, 2010, **463**, 789-792.
53 K. Noda, K. Ishida, A. Kubono, T. Horiuchi, H. Yamada and K. Matsushige, *J. Appl. Phys.*, 2003, **93**, 2866-2870.
54 M. Szafrański, A. Katrusiak and G. J. McIntyre, *Phys. Rev. Lett.*, 2002, **89**, 215507.
55 S. Hoshino, T. Mitsui, F. Jona and R. Pepinsky, *Phy. Rev.*, 1957, **107**, 1255.
56 M. Szafrański, *J. Phys. Chem. B*, 2011, **115**, 8755-8762.
57 D.-W. Fu, H.-L. Cai, Y. Liu, Q. Ye, W. Zhang, Y. Zhang, X.-Y. Chen, G. Giovannetti, M. Capone, J. Li and R. G. Xiong, *Science*, 2013, **339**, 425-428.
58 D.-W. Fu, W. Zhang, H. L. Cai, J. Z. Ge, Y. Zhang and R. G. Xiong, *Adv. Mater.*, 2011, **23**, 5658-5662.
59 H. Ma, W. Gao, J. Wang, T. Wu, G. Yuan, J. Liu and Z. Liu, *Adv. Electron. Mater.*, 2016, **2**, 1600038.
60 L. E. Cross, *Relaxor Ferroelctrics*. In *Piezoelectricity: evolution and future of a technology*. Vol. 114, Springer Science & Business Media, 2008, 131-155.
61 A. A. Bokov and Z.-G. Ye, *J. Adv. Dielectr.*, 2012, **2**, 1241010-1-24.
62 The [[Hy-Na]⊂**1**]) did not give a well-saturated loop and hence it is not included in any of the ferroelectric related discussions.
63 G.-C. Xu, W. Zhang, X.-M. Ma, Y.-H. Chen, L. Zhang, H.-L. Cai, Z.-M. Wang, R.-G. Xiong and S. Gao, *J. Am. Chem. Soc.*, 2011, **133**, 14948–14951.
64 F. R. Fan, W. Tang and Z. L. Wang, *Adv. Mater.*, 2016, **28**, 4283–4305.

View Article Online
DOI: 10.1039/C7TC01758H

Table of Contents Entry

Altering Polarization Attributes in Ferroelectric Metallo-Cavitands by Varying Hydrated Alkali-Metal Guest Cations

Anant Kumar Srivastava, Thangavel Vijayakanth, Pillutla Divya, B. Praveenkumar,* Alexander Steiner* and Ramamoorthy Boomishankar*

Synthesis two new chiral metal-ligand cavitands $[\{Ni_4L_8(H_2O)_8\}\supset 9(H_2O)]\cdot 8(NO_3)\cdot 25(H_2O)$ (**1**) and $[\{Co_4L_8(H_2O)_8\}\supset 9(H_2O)]\cdot 8(NO_3)\cdot 27(H_2O)$ (**2**) have been reported. Both **1** and **2** encapsulate various hydrated alkali metal cations (Hy-A) at their intrinsic voids with relatively high hydration numbers. Ferroelectric studies on **1**, [Hy-A]⊂**1** and [Hy-A]⊂**2** assemblies show high remnant polarization (P_r) values with guest-dependent variations in their polarization attributes.